Journal of Catalysis **192,** 400–411 (2000)
doi:10.1006/jcat.2000.2862, available online at http://www.idealibrary.com on IDEAL®

Effect of Grafting Sequence on the Behavior of Titania-Supported V_2O_5–WO_3 Catalysts in the Selective Reduction of NO by NH_3

M. A. Reiche,* P. Hug,† and A. Baiker*,[1]

*Laboratory of Technical Chemistry, Swiss Federal Institute of Technology, ETH-Zentrum, CH-8092 Zürich, Switzerland; and †EMPA, Ueberlandstrasse 129, 8600 Dübendorf, Switzerland

Received November 15, 1999; revised March 3, 2000; accepted March 3, 2000

V_2O_5–WO_3/TiO_2 catalysts have been prepared by subsequent, alternating, and simultaneous grafting of vanadia and tungsta onto titania. The performance of these catalysts in the selective catalytic reduction (SCR) of NO by NH_3 was compared with corresponding titania-supported single oxides prepared by the same method. For a given composition, the activity of the catalysts depended only marginally on the sequence of grafting for catalysts with low loadings (up to an experimental monolayer, ca. 10 μmol V/m^2 and 6 μmol W/m^2, respectively). Increase of the calcination temperature from 573 to 773 K decreased the activity of catalysts with low loading. This behavior is attributed to spreading of the vanadia species over the titania surface, resulting in an increase of less active monomeric vanadyl species. For catalysts with higher loading (>experimental monolayer), the interaction between vanadia and tungsta species was intensified with increasing calcination temperature, affording higher activity and new species with hydroxyl groups characterized by an IR-band at a frequency $\leq$3600 cm^{-1}. The formation of weaker acid sites from which ammonia desorbed at temperatures <500 K was found to be correlated to SCR activity. In contrast, no correlation was observed between the activity and the ease of reduction of the catalysts by ammonia. TOF-SIMS measurements indicated that V–O–W connectivities were present on the V_2O_5–WO_3/TiO_2 catalysts, indicating strong interaction between vanadia and tungsta species, which results in a higher activity compared to the corresponding titania-supported single oxides. The studies demonstrate that high activity can be achieved with ternary V_2O_5–WO_3/TiO_2 catalysts if the total loading exceeds an experimental monolayer and the catalyst is calcined at 773 K, or with catalysts derived from WO_3/TiO_2 calcined at 1023 K before vanadia deposition. © 2000 Academic Press

Key Words: vanadia; tungsta; titania; grafting; nitric oxide; selective reduction; ammonia; temperature-programmed reduction; temperature-programmed desorption; DRIFTS.

1. INTRODUCTION

Various methods for the preparation of vanadia-based catalysts suitable for the selective catalytic reduction (SCR) of NO by NH_3 have been reported (1, 2). Commercial SCR catalysts are mostly based on vanadia/titania and often contain considerable amounts of tungsten oxide and/or molybdenum oxide (3). Numerous investigations exist on binary V_2O_5/TiO_2 catalysts (1–5), whereas much less work has been expended on ternary V_2O_5–WO_3/TiO_2 catalysts. Typically, ternary V_2O_5–WO_3/TiO_2 catalysts are prepared by means of the incipient wetness (6–8) or wet impregnation method (9). Grafting of vanadium alkoxides on TiO_2 and TiO_2–SiO_2 oxides allows good control of the vanadium loading in the submonolayer range (2, 10–12). This beneficial feature can be utilized to explore the interaction between grafted vanadia and tungsta species in ternary V_2O_5–WO_3/TiO_2 catalysts with low and high loading.

An important, but still unanswered, question is how the sequence of the metal alkoxide graftings influences the structural and catalytic properties of as-prepared ternary catalysts. With this in mind we have prepared a series of binary (V_2O_5/TiO_2, WO_3/TiO_2) and ternary (V_2O_5–WO_3/TiO_2) catalysts. The ternary catalysts were prepared by sequential, alternating, and simultaneous grafting. The main target was to elucidate the influence of the grafting sequence of vanadia and tungsta on the catalyst properties. Catalyst preparation together with some structural properties investigated by inductive coupled plasma atom absorption spectroscopy (ICP-AAS), N_2-physisorption, X-ray diffraction (XRD), laser Raman spectroscopy (LRS), X-ray photoelectron spectroscopy (XPS), temperature-programmed reduction (TPR) in hydrogen, and diffuse reflection infrared Fourier transform spectroscopy (DRIFTS) have been the focus of a previous study (13).

Here we extend the structural characterization of these catalysts and describe their use in the selective catalytic reduction of NO by NH_3. Characterization of the catalysts by temperature-programmed desorption (TPD), DRIFTS, TPR with NH_3, and time of flight secondary ion mass spectrometry (TOF-SIMS) were applied to elucidate the relationship between surface properties and activity of the catalysts.

[1] To whom correspondence should be addressed. E-mail: baiker@tech.chem.ethz.ch.

0021-9517/00 $35.00

2. EXPERIMENTAL

2.1. Catalyst Preparation

Preparation of the differently grafted catalysts and their structural characterization by ICP-AAS, N_2-physisorption, XRD, LRS, XPS, TPR with hydrogen, and DRIFTS have been described in detail in (13). In brief, the TiO_2 support (P25, particle size 0.3–0.5 mm) was exposed to a precursor solution of either vanadyl triisopropoxide (VOTIP) or 0.24 mmol tungsten (V) ethoxide in water-free tetrahydrofuran (THF). After the solution was removed, the catalyst was washed with fresh tetrahydrofurane, dried, and finally calcined in dry oxygen at 573 K for 3 h. Higher loading was achieved by repeating the grafting procedure. To compensate for the higher reactivity of the vanadium alkoxide, a molar ratio of V : W precursor of 1 : 4 was used for the simultaneous grafting.

The catalysts are referred to as "m_1M_1/m_2M_2" where m_1 and m_2 represent the number of grafting steps with the corresponding metal precursor M_1 or M_2. The slash indicates that M_2 was deposited after M_1. A subscript indicates the calcination temperature, which is only specified if it is higher than the standard calcination temperature of 573 K. For example, $5W_{1023}/3V$ means that the catalyst 5W was calcined at 1023 K before it was triply grafted with vanadia. Note that m(W/V) represents all catalysts of the alternatingly grafted series, e.g., W/V, WV/W, WVW/V, WVWV/W, and WVWVW/V. For simultaneous grafting of vanadia and tungsta m(W + V) is used.

2.2. Catalyst Characterization

DRIFTS. DRIFT spectra were recorded on a Perkin–Elmer 2000 NIR-FT-Raman spectrometer using a diffuse reflection cell (Spectra Tech 003-102) equipped with CaF_2 windows. The powdered samples were calcined *in situ* in 7.2% O_2/Ar (50 ml min^{-1}) for 1 h at 573 or 723 K, respectively. Afterward, background spectra were recorded at decreasing temperature. The catalysts were then exposed to an SCR feed gas mixture (see catalytic tests), heated to 573 K, cooled to 323 K, and subsequently purged in an Ar flow (50 ml min^{-1}) for 1 h. Adsorbed species were desorbed by increasing the temperature. The recorded spectra were displayed in Kubelka–Munk units with the calcined catalyst as background.

TPR. NH_3-TPR experiments were performed in a continuous-flow fixed-bed quartz microreactor with 4 mm internal diameter. Volumes of 0.126 cm^3, corresponding to 35–75 mg of catalyst granules, were used for the measurements. The catalysts were pretreated *in situ* in 50 ml min^{-1} 7.2% O_2/He for 3 h at 573 or 773 K, respectively. After cooling to room temperature, 3600 ppm NH_3/He was passed over the catalyst bed for 1 h, and then the temperature was raised at 10 K min^{-1} to 723 or 773 K, respectively. The concentrations of NH_3 and the products of NH_3 oxidation, H_2O, NO, N_2, and N_2O, were monitored by mass spectrometry (MS).

TPD. SCR-TPD experiments were performed *in situ* with the same sample and apparatus as used for the catalytic tests (see below). SCR feed gas (50 ml min^{-1}) was passed through the catalyst bed at 300 K for 45 min after complete SCR testing (20 h, see below). After purging for 1.5 h with He (99.999%, 50 ml min^{-1}), the temperature was raised at 10 K min^{-1} to 773 K and the concentrations of the evolving species H_2O, NH_3, NO, N_2, and N_2O were monitored by mass spectrometry (MS). For ternary catalysts after calcination at 573 K burning of organic residues at temperatures higher than 623 K can not be excluded. This can result in an enhancement of the nitrogen (due to fragments of CO and CO_2 at $m/z = 28$) and water signal at temperature >623 K.

TOF-SIMS. Positive and negative secondary ion mass spectra were recorded with a Physical Electronics Model 7200 instrument. The spectrometer was equipped with a pulsed Cs primary ion gun. The gun was delivering Cs^+-pulses with an energy of 8 kV and a pulse width of less than 1 ns. This resulted in a mass resolution $M/\Delta M$ of more than 5000 at mass $m/z = 28$. The sample particles were attached to a standard sample holder with a pad of a conductive adhesive. Charging of the sample was neutralized with an electron flood gun. During experiments the ion beam was rastered over an area of 300×300 μm and the ion doses were kept well below the static SIMS limit of 10^{13} ion/cm^2.

Catalytic tests. Studies of SCR of NO by NH_3 were carried out in a continuous-flow fixed-bed quartz microreactor with 4 mm internal diameter. Volumes of 0.126 cm^3 corresponding to 35–75 mg of catalyst granules were used for the measurements. Before activity tests, the catalysts were pretreated *in situ* in 50 ml min^{-1} 7.2% O_2/He for 3 h at 573 or 773 K, respectively. The reaction gas mixture consisted of 900 ppm NO, 900 ppm NH_3, and 1.8% O_2 in a helium balance. This gas mixture, which is referred to as the SCR feed, was mixed from He (99.999%) and single component gases in an He balance (3600 ppm NO/He, 3600 ppm NH_3/He certified by ±2%, Carba Gas). Feed and product concentrations of NO, NO_2, NH_3, H_2O, N_2O, O_2, and N_2 were quantitatively analysed on-line using a Balzers quadrupole mass spectrometer QMG 420 equipped with an QMA 125 analyser with 90° off axis SEV detector.

Conversion measurements as a function of temperature were carried out at a gas hourly space velocity, GHSV, of ca. 24,000 h^{-1} (referred to total bed volume) between 380 and 623 K in steps of 15 K. For activity measurements, the space velocity was gradually raised from 17,000 to 85,000 h^{-1} and the temperature was adjusted to keep the NO conversion between 14 and 20% in order to maintain conditions close to differential reactor conditions. For

integral and differential runs, steady-state conditions were monitored after 30 min at each temperature. Selectivities to N_2 and N_2O were defined as $S_i = F_i/(F_{N_2} + F_{N_2O})$, where F_i is the molar flow rate (mol/s) of species i (N_2 or N_2O) at the reactor outlet. NO_2 was not observed in any run. However, decomposition at the cathode of some NO_2 formed cannot be ruled out completely. The criterion of Weisz and Prater (14) ($Da = -r_{obs}R^2/(D_{eff}C_g < 1)$ was used to estimate the possible influence of internal mass transfer. For $5W_{1023}/3V$ the Damköhler number was calculated to be $Da = 0.8$ at $T = 470$ K ($r_{NO}/C_{NO} = 5.48\ s^{-1}$, $R = 0.25$ mm, $D_{NO} = 4.3\ 10^{-7}\ m^2\,s^{-1}$), indicating that pore diffusion was not limiting at temperatures <470 K. This is further corroborated by measurements with V_2O_5/TiO_2 aerogels with similar reactivity but higher pore volume and lower mean pore diameter. There the kinetic data were independent of the particle size (<500 μm) between 395 and 440 K (15). Thus the majority of the kinetic tests were run at temperatures lower than 470 K.

For all measurements a nitrogen balance including feed and product stream concentrations of all nitrogen-containing compounds was calculated. Even for high conversions of NO and NH_3 the error in the N-balance did not exceed ±5%.

3. RESULTS

Preliminary investigations indicated that, depending on the loading, the grafting sequence has a different effect on structural and catalytic properties of the catalysts. Consequently we have structured the presentation of the results by distinguishing three ranges of loading. In section A the catalysts with a total loading (V + W) of less than an experimental monolayer are presented. Note that different suggestions concerning the experimental monolayer (referred to as the monolayer throughout the paper) are reported in the literature, depending on the measuring technique used (2, 16–20). Here we use the values assigned by XPS determined in our previous work (13), corresponding to ca. 10 μmol V/m^2 and 5–6 μmol W/m^2, respectively. Section B concerns catalysts with a total loading of about a monolayer, and in section C catalysts with loadings exceeding a monolayer are discussed. In the final section, D, we address catalysts derived from WO_3/TiO_2 calcined at 1023 K before grafting with vanadia.

3.1. Catalytic Behavior in the Selective Reduction of NO with NH_3

For all ternary catalysts the N_2O production was generally not significant up to 573 K; only with catalysts of higher vanadia loading (three graftings with vanadia) and after calcination at low temperature (573 K) were significant amounts of N_2O found, but always lower than 11 ppm ($S_{N_2O} < 1.2\%$) at 573 K.

TABLE 1

SCR-DeNO$_x$ on V_2O_5/TiO_2 and WO_3–V_2O_5/TiO_2 Catalysts: Turnover Frequencies (TOF) at 423 K and Apparent Activation Energy (E_a)

Catalyst	Loading (μmol/m^2)		T_{calc} (K)	S_{BET} (m^2/g)	TOF (NO/(V*ks))	E_a (kJ/mol)
1V	3.8[a]		573	50	0.10	68 ± 2[c]
			773	42	0.05	68 ± 2
2V	6.6		573	48.4	0.35	65 ± 2
			773	40.5	0.33	65 ± 1
3V	8.3		573	48.1	0.47	66 ± 2
			773	40.2	0.42	66 ± 2
4V	10.1		573	46.6	0.48	60 ± 3
			773	40.1	0.46	65 ± 3
2V/1W	5.6	1.2[b]	573	47.2	0.38	67 ± 6
			773		0.30	68 ± 2
2V/2W	5.0	2.6	573	46.2	0.43	66 ± 5
			773		0.43	67 ± 2
4V/1W	8.9	0.9	573	46.2	0.47	60 ± 2
			773	40.0	0.42	62 ± 3
4V/2W	7.8	2.1	573	45.5	0.45	61 ± 1
			773	39.5	0.49	62 ± 3
4V/3W	7.3	3.6	573	44.7	0.45	59 ± 4
			773	39.7	0.58	59 ± 2

[a] V loading in μmol V/m^2.
[b] W loading in μmol W/m^2.
[c] Ninety-five percent confidence limits of Arrhenius type linear regression.

Table 1 lists the catalytic results for the binary V_2O_5/TiO_2 catalysts. Up to the third grafting the intrinsic activity (TOF, Table 1) increased with vanadia loading for V_2O_5/TiO_2 catalysts and then remained constant, in line with the literature (21). Also, the values of the apparent activation energy of 64 ± 5 kJ/mol agree well with literature values (22).

The catalyst 4V and some ternary catalysts were tested in the SCR from 300 K on; already at this temperature a conversion to nitrogen and water of ca. 1% could be observed. This observation corroborates the finding of Hu and Apple (23), who reported SCR activity for V_2O_5/TiO_2 catalysts at room temperature.

A. Catalysts with a total loading of less than a monolayer. Note that for all ternary catalysts the TOF values are referred to the total amount of vanadium. As the binary WO_3/TiO_2 catalysts were only active at temperatures above ca. 500 K, it was assumed that the W sites in the ternary catalysts were not significantly active in the catalytic reaction at 423 K. Ternary catalysts of low total loading and vanadia loading ≤3 μmol V/m^2 (2W/1V, W/V, WV/W, m(W + V)) exhibited only low intrinsic activity (TOF ≤ 0.26 NO/(V*ks), Tables 2 and 3). These catalysts also showed high activation energies (ca. 79 kJ/mol, Tables 2 and 3). Catalyst 2V/1W with higher V loading was more active (Table 1); its activation energy was in the range of that of the binary V_2O_5/TiO_2 catalysts.

TABLE 2

SCR-DeNO$_x$ on V_2O_5–WO_3/TiO_2 Catalyst: Turnover Frequencies (TOF) at 423 K and Apparent Activation Energy (E_a)

Catalyst	Loading (μmol/m^2)		T_{calc} (K)	S_{BET} (m^2/g)	TOF (NO/(V*ks))	E_a (kJ/mol)
2W/1V	2.7[a]	3.0[b]	573	48.4	0.18	79 ± 3[c]
			773	43.5	0.16	72 ± 2
2W/2V	4.6	3.0	573	48.2	0.43	68 ± 2
			773	41.2	0.43	63 ± 2
2W$_{1023}$/1V	2.8	5.2[d]	573	28.2	0.53	68 ± 4
			773	25.5	0.37	66 ± 2
2W$_{1023}$/2V	4.4	5.3[d]	573	27.7	0.67	62 ± 3
			773	24.3	0.54	60 ± 3
5W/1V	2.3	6.0	573	46.6	0.21	68 ± 2
			773	43	0.42	64 ± 1
5W/2V	3.9	6.0	573	45.7	0.35	64 ± 3
			773	40.4	0.59	60 ± 4
5W/3V	5.5	6.0	573	44.7	0.42	62 ± 2
			773	39.3	0.66	56 ± 1
5W$_{1023}$/1V	2.3	8.0[d]	573	35	0.62	54 ± 2
			773	31.9	0.68	56 ± 5
5W$_{1023}$/2V	3.6	7.8[d]	573	34.9	0.57	57 ± 3
			773	30.1	0.72	55 ± 1
5W$_{1023}$/3V	5.2	7.9[d]	573	34.7	0.47	55 ± 2
			773	30.7	0.62	53 ± 1
			823	30.6	0.62	52 ± 2
			873	30.5	0.65	50 ± 2
			900	29.0	0.65	49 ± 4

[a] V loading in μmol V/m^2.

[b] W loading in μmol W/m^2.

[c] Ninety-five percent confidence limits of Arrhenius type linear regression.

[d] Not representing the loading at the surface because enclosing of W during sintering is not considered.

Increasing the calcination temperature from 573 (standard) to 773 K resulted in a decrease of activity for all low loaded catalysts (TOF, Tables 1–3). The activation energy decreased for all catalysts, except 2V/1W, which already exhibited low activation energy after calcination at 573 K.

B. Catalysts with a total loading of about a monolayer. For the ternary catalysts with similar V and W loadings, 2V/2W, 2W/2V, and WVW/V, no significant differences in the intrinsic activity (TOF = 0.43–0.47 NO/(V*ks), Tables 1–3) or in the activation energy were observed. The activation energy was in the range of the binary V_2O_5/TiO_2 catalysts, and turnover frequencies were similar to those of the high loaded V_2O_5/TiO_2 catalysts. Note that the loading of catalysts 4V/1W and 4V/2W was also about a monolayer due to dissolution of vanadia during the preparation process (13). For these two catalysts the same activity (TOF, Table 1) was found as for the other catalysts with monolayer loading. All monolayer catalysts showed no significant change in activity or activation energy when the calcination temperature was increased from 573 to 773 K (Tables 1–3).

C. Catalysts with a total loading exceeding a monolayer. For the alternatingly grafted catalysts the intrinsic activity (TOF, Table 3) increased with the total metal loading up to the fourth grafting (approximately monolayer coverage) independent of the last grafting step (vanadia or tungsta). However, it slightly decreased with the fifth and sixth grafting (WVWV/W and WVWVW/V) when exceeding a monolayer. In contrast, for the catalysts 5W/mV, where vanadia was grafted onto WO_3/TiO_2, the intrinsic activity increased with the vanadia loading when exceeding monolayer coverage (Table 2). For 4V/3W no change in intrinsic activity was observed compared to the lower loaded samples of this series. The activation energy was lowest for 4V/3W (59 kJ/mol) and 65 ± 3 kJ/mol for the other catalysts.

Increasing the calcination temperature from 573 to 773 K enhanced the intrinsic activity for all high loaded catalysts between 30 and 100%. Highest TOF was found for 5W/3V. With the exception of 4V/3W, the activation energy decreased and was only 56 kJ/mol for the catalysts with the highest loadings (5W/3V and WVWVW/V).

D. Catalysts derived from WO_3/TiO_2 calcined at 1023 K. Calcination of WO_3/TiO_2 catalysts at 1023 K resulted in significantly higher activity compared to their calcination at 573 K as previously found (24, 25). The catalysts m_1W_{1023}/m_2V showed markedly different behavior in comparison to the corresponding catalysts m_1W/m_2V, reflected by higher activity and lower activation energy (Table 2). After single grafting with vanadia the TOF was three times higher for 2W$_{1023}$/1V and 5W$_{1023}$/1V than for 2W/1V

TABLE 3

SCR-DeNO$_x$ on Alternatively and Simultaneously grafted V_2O_5–WO_3/TiO_2 Catalyst: Turnover Frequencies (TOF) at 423 K and Apparent Activation Energy (E_a)

Catalyst	Loading (μmol/m^2)		T_{calc} (K)	S_{BET} (m^2/g)	TOF (NO/(V*ks))	E_a (kJ/mol)
W/V	3.0[a]	1.8[b]	573	49.8	0.13	80 ± 3[c]
			773	42.3	0.09	69 ± 1
WV/W	2.8	3.2	573	48.8	0.26	75 ± 2
			773	42.4	0.19	71 ± 2
WVW/V	4.7	3.3	573	47.8	0.47	69 ± 2
			773	42.3	0.48	66 ± 3
WVWV/W	4.5	4.8	573	46.2	0.44	68 ± 2
			773	41.6	0.58	60 ± 4
WVWVW/V	6.3	4.8	573	44.5	0.40	65 ± 3
			773	38.0	0.61	56 ± 3
1(W + V)	1.1	1.2	573	50.0	0.01	
2(W + V)	1.9	2.1	573	50.0	0.06	
			773		0.04	
3(W + V)	2.3	2.4	573	49.8	0.12	79 ± 3
			773	43.0	0.07	69 ± 2

[a] V loading in μmol V/m^2.

[b] W loading in μmol W/m^2.

[c] Ninety-five percent confidence limits of Arrhenius type linear regression.

and 5W/1V, respectively. Whereas for $2W_{1023}/2V$ a further increase with the second grafting was observed, for $5W_{1023}/mV$ the intrinsic activity decreased with vanadia loading. The activation energy for catalysts $2W_{1023}/mV$ was in the range of that of the catalysts with loadings of a monolayer or more, whereas $5W_{1023}/mV$ exhibited a lower activation energy (55 ± 2 kJ/mol, Table 2).

For $2W_{1023}/mV$, TOF decreased when the catalyst was calcined at 773 K, as observed with the low loaded catalysts. In contrast, for $5W_{1023}/2V$ and $5W_{1023}/3V$ the intrinsic activity increased significantly, as found for the high loaded ternary catalysts. No significant change in the activation energy was observed when the calcination temperature was increased. $5W_{1023}/3V$ showed no significant change in activity or activation energy when calcined between 773 and 900 K (Table 2).

For all ternary catalysts, of this study activities (TOFs) at 423 K were higher than for the binary V_2O_5/TiO_2 catalysts with corresponding vanadia loading.

3.2. Surface Chemical Properties

The catalysts were characterized by various methods, including ICP-AAS, N_2-physisorption, XRD, LRS, XPS, and TPR in hydrogen. The results of these investigations have been reported together with the catalyst preparation in a previous publication (13). Here we extend the characterization to SCR-TPD, DRIFTS, TPR in ammonia, and TOF-SIMS investigations.

3.2.1. Temperature-Programmed Desorption (SCR-TPD)

TPD investigations were carried out after catalytic measurements and cooling of the samples in SCR feed gas to 300 K, loading with SCR feed gas, and purging with He, as described under Experimental.

TiO_2 and binary WO_3/TiO_2 reference catalysts. In Fig. 1 the desorption profiles are shown for the pure titania support P25 and WO_3/TiO_2 catalysts. A strong water desorption with maximum at 440 K was observed for P25, which decreased in intensity with increasing tungsta loading and shifted to 380 K for 5W. A second water desorption maximum of P25 appeared at 650 K, together with maxima of N_2 and NO evolution. With increasing tungsta loading a weak water maximum developed around 700 K. P25 showed NH_3 desorption maxima at 375 and 560 K. Both maxima decreased with increasing tungsta loading, and new maxima developed around 480 and 670 K. The strong N_2 evolution at 400 K observed for P25 decreased in intensity with increasing tungsta loading and shifted to 360 K for 5W.

For all WO_3/TiO_2 catalysts, increasing the calcination temperature from 573 to 1023 K resulted in reduced NH_3 desorption, whereas the position of the maxima did not change. The amount of evolving nitrogen decreased.

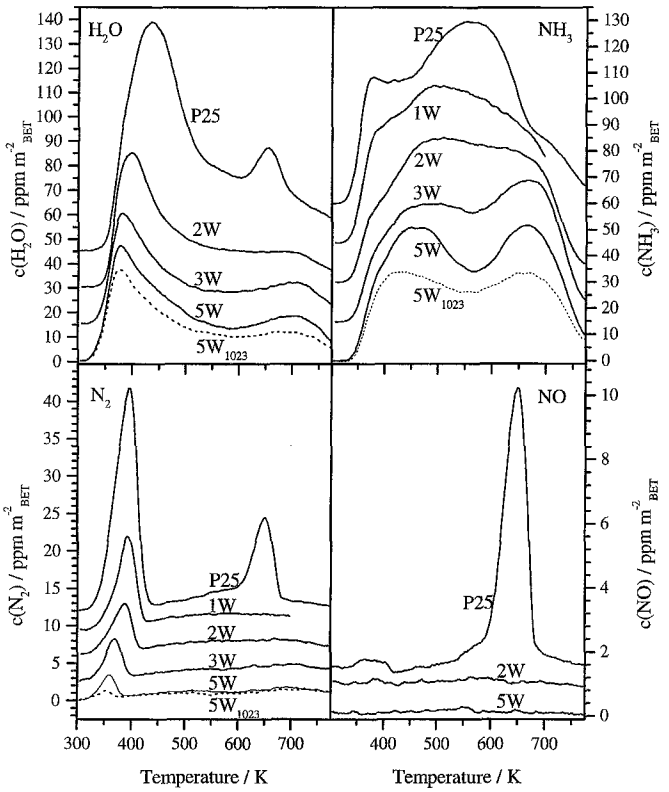

FIG. 1. Influence of tungsta loading on TPD profiles of pure titania support (P25) and WO_3/TiO_2 (mW) catalysts. Desorption curves of H_2O, NH_3, N_2, and NO measured after catalytic testing up to 573 K and subsequent exposure to SCR feed at room temperature (SCR-TPD). The concentrations are referred to the total surface area (BET) of the samples. TPD in flowing He (50 ml/min, STP); sample bed volume, 0.126 ml; heating rate, 10 K/min. Sample designations are explained under Experimental.

Binary V_2O_5/TiO_2 reference catalysts. Desorption profiles for the V_2O_5/TiO_2 catalysts (Fig. 2) were greatly different from those of the pure titania support (P25) and the WO_3/TiO_2 catalysts. Instead of the dominant water desorption at 440 K only a weak water desorption at 380 K was observed for the singly grafted catalyst 1V. A water maximum at 680 K was accompanied by nitrogen evolution. NH_3 desorption was shifted toward higher temperature compared to P25, with a plateau spanning from 420–470 K and a maximum at ca. 630 K. The N_2 evolution at 360 K, observed for P25 and WO_3/TiO_2 catalysts, was only weak, but new small N_2 and NO evolutions occurred around 470 K. Distinct changes appeared with the second grafting, whereas with the third and fourth graftings the changes were less pronounced. The first water maximum increased with higher vanadia loading. Starting with the second grafting a shoulder developed at 420 K together with maxima of N_2 and NO evolution. Further water maxima were observed at 495 (2V) and 480 K (3V, 4V), respectively. Interestingly, at the same temperatures NH_3 maxima were also observed. The water and N_2 evolutions at 680 K were shifted to 580 K for

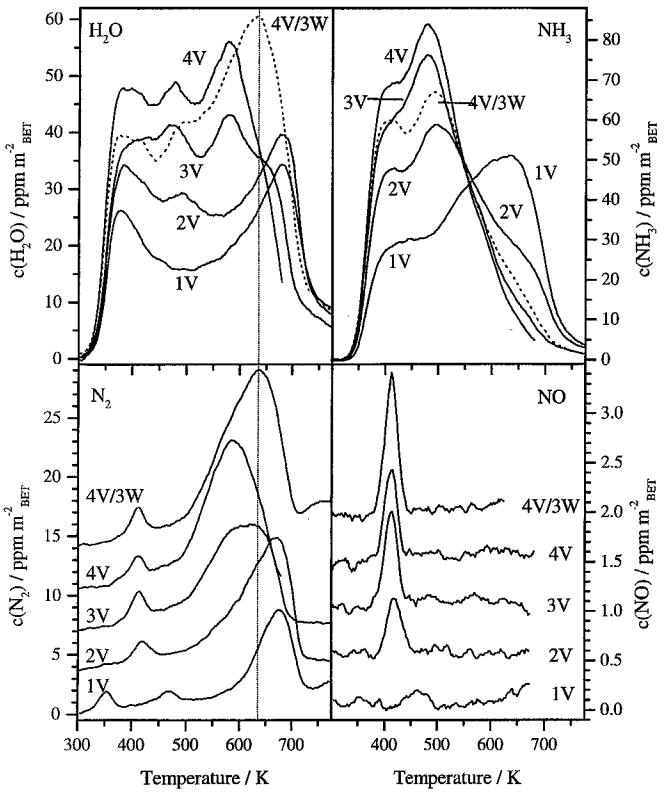

FIG. 2. Influence of vanadia and tungsta loading on TPD profiles of V_2O_5/TiO_2 (mV) and WO_3–V_2O_5/TiO_2 (4V/3W) catalysts. Desorption curves of H_2O, NH_3, N_2, and NO measured after catalytic testing up to 573 K and subsequent exposure to SCR feed at room temperature (SCR-TPD). Same conditions as in Fig. 1.

3V and 4V. In the NH_3 desorption curve both the maximum at 480 K and a shoulder at ca. 410 K increased with higher vanadia loading.

Increasing the calcination temperature from 573 to 773 K had only a minor influence on the shape of the desorption profiles, but the amount of desorbing ammonia per m^2 increased by ca. 10–20%. For water, N_2, and NO, slight increases were also observed.

A. Catalysts with a total loading of less than a monolayer. The TPD profiles of the ternary catalysts (Figs. 3 and 4) of low total loading and vanadia loading ≤ 3 μmol V/m^2 (2W/1V, W/V, WV/W, m(W + V)) exhibited characteristics similar to those of the singly grafted V_2O_5/TiO_2 catalyst 1V (cf. Fig. 2). As for the activity (Tables 1–3), catalyst 2V/1W differed from the other low loaded catalysts and showed profiles similar to those of catalyst 2V.

When catalysts were calcined at 773 K instead of 573 K, the NH_3 desorption maximum around 550–600 K shifted toward higher temperature (ca. 20 K, not shown).

B. Catalysts with a total loading of about a monolayer. All catalysts with about monolayer loading (2V/2W, 2W/2V, WVW/V, 4V/1W, and 4V/2W) exhibited desorption profiles similar to those of the multiply grafted binary V_2O_5/TiO_2 catalysts with two NH_3 maxima at 400 and 500 K, and only weak desorption above 550 K (compare 2W/2V and WVW/V in Figs. 3 and 4). Besides the water maximum at 375 K, shoulders or maxima around 415, 505, and 630 K were observed. These maxima coincided with maxima of N_2 (415, 630 K), NO (415 K), and NH_3 evolution (500 K), respectively.

No significant shift in the NH_3 desorption maxima was observed when the calcination temperature was increased from 573 to 773 K (not shown).

C. Catalysts with a total loading exceeding a monolayer. Grafting of tungsta onto V_2O_5/TiO_2 had little influence on the desorption profiles. For 4V/3W (Fig. 2), a decrease of the amount of adsorbed ammonia was observed, compared to that of 4V, and the NH_3 maxima became more distinct. Whereas the water maxima at 380 K decreased in intensity, the water maximum as well as the nitrogen maximum at higher temperature grew in intensity and shifted to 635 K.

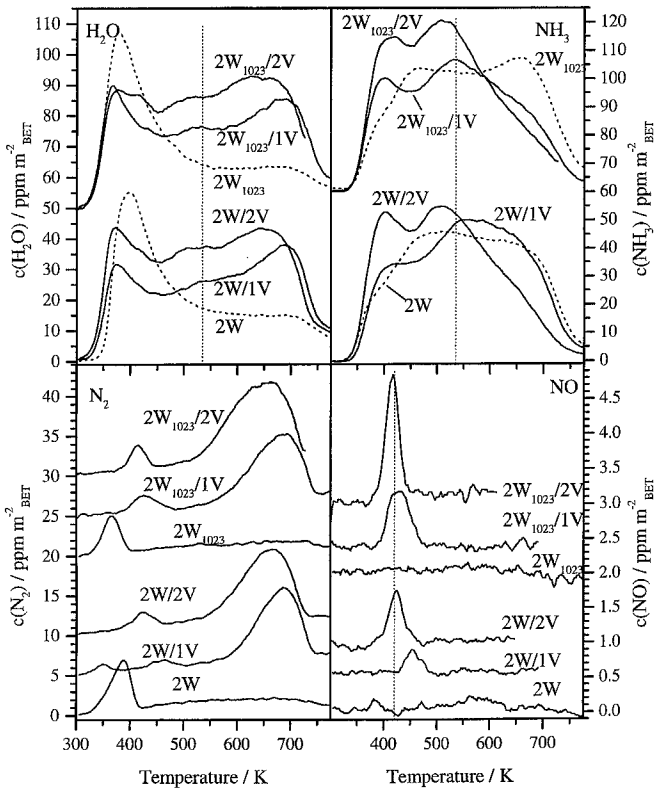

FIG. 3. Influence of calcination temperature on TPD profiles of WO_3/TiO_2 catalysts (2W calcined at 573 K and $2W_{1023}$ calcined at 1023 K) and corresponding catalysts grafted with vanadia (2W/mV and $2W_{1023}$/mV). Desorption curves of H_2O, NH_3, N_2, and NO measured after catalytic testing up to 573 K and subsequent exposure to SCR feed at room temperature (SCR-TPD). The V_2O_5–WO_3/TiO_2 catalysts with corresponding number of graftings had equivalent vanadia loading per surface area. Same conditions as in Fig. 1.

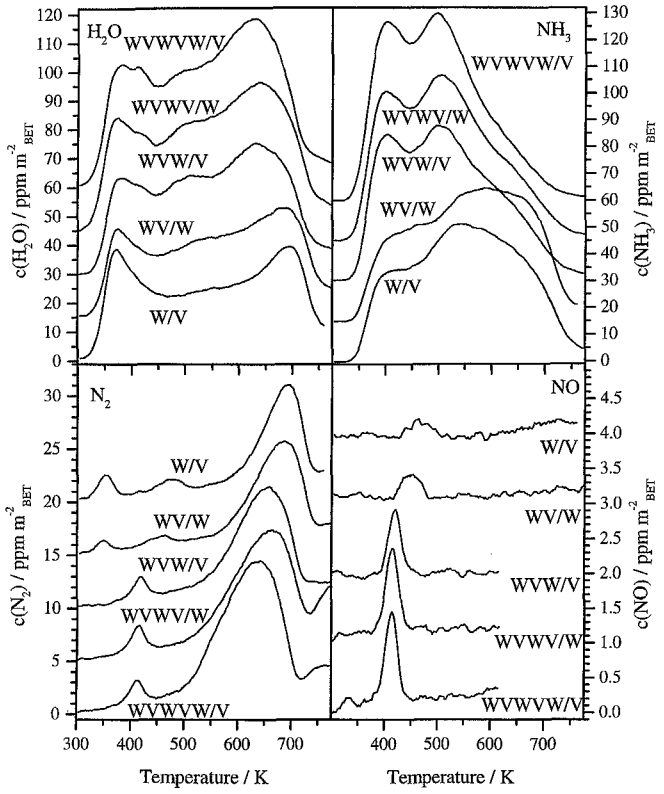

FIG. 4. Influence of alternating grafting with tungsta and vanadia on the TPD profiles of WO_3–V_2O_5/TiO_2 (mW/V) catalysts. Desorption curves of H_2O, NH_3, N_2, and NO measured after catalytic testing up to 573 K and subsequent exposure to SCR feed at room temperature (SCR-TPD). Same conditions as in Fig. 1.

The 5W/mV series showed two NH_3 maxima (not presented), one at low temperature (400 K) and the other shifting from 550 to 500 K with increasing vanadia loading. The amount of ammonia desorbing below 500 K increased, whereas that above 500 K decreased with increasing vanadia loading. Water maxima at 380 K and around 500–550 K behaved similarly. Weak H_2O, N_2, and NO maxima at ca. 420 K, and strong water and N_2 maxima around 670 K, were observed, the latter shifting to lower temperature with increasing vanadia loading.

For the alternatingly grafted catalysts with the fifth and sixth graftings no significant changes in the form of the TPD profiles occurred compared to those of WVW/V; only the amount of desorbing ammonia increased with the sixth grafting (Fig. 4).

Increasing the calcination temperature from 573 to 773 K resulted in a shift (ca. 15 K) of the NH_3 and H_2O maximum around 500 K to lower temperature for all catalysts with a total loading exceeding a monolayer. N_2 and NO evolutions at ca. 415 K increased in intensity. The decrease in the intensity of water and $m/z = 28$ signal at $T > 623$ K can be attributed to the burning of organic residues during calcination at 773 K.

D. Catalysts derived from WO_3/TiO_2 calcined at 1023 K. Catalyst $2W_{1023}$/1V showed more pronounced changes in the NH_3 desorption compared to $2W_{1023}$ than 2W/1V compared to 2W, indicating a significant effect of calcination at 1023 K before vanadia grafting. For $2W_{1023}$/1V the NH_3 desorption profile (Fig. 3) was similar to that for the multiply grafted V_2O_5/TiO_2 catalysts (Fig. 1); this contrasts with the behavior of 2W/1V with a profile (Fig. 3) resembling that of 1V (Fig. 1). Similar but less pronounced differences were observed for the catalysts 5W and $5W_{1023}$ grafted with vanadia (not shown). After the second grafting with vanadia the desorption profiles became similar (compare $2W_{1023}$/2V and 2W/2V in Fig. 3).

With higher calcination temperature (773 K), the NH_3 desorption maximum above 500 K shifted ca. 20 K to higher temperature for $2W_{1023}$/1V, whereas for $2W_{1023}$/2V and $5W_{1023}$/mV no significant shift in the NH_3 desorption maximum was observed. For all catalysts the water and N_2 evolution around 650 K decreased in intensity.

Generally it can be stated that for all catalysts, independent of the sequence of grafting, the changes in the TPD profiles after the grafting of vanadia were more pronounced than those after the grafting of tungsta.

3.2.2. *Diffuse Reflectance Infrared Fourier Transform Spectroscopy (DRIFTS)*

Acid centers detected by DRIFTS after exposure to SCR conditions. Adsorbed ammonia gives rise to several bands in infrared spectra. Bands between 3400 and 3150 cm^{-1} and around 1600 and 1200 cm^{-1} are assigned to Lewis bound ammonia. Bands around 3000, 2800, 1680, and 1450 cm^{-1} are assigned to Brønsted bound ammonia (26–28). Figure 5 shows the DRIFT spectra after exposure of catalyst 5W/3V

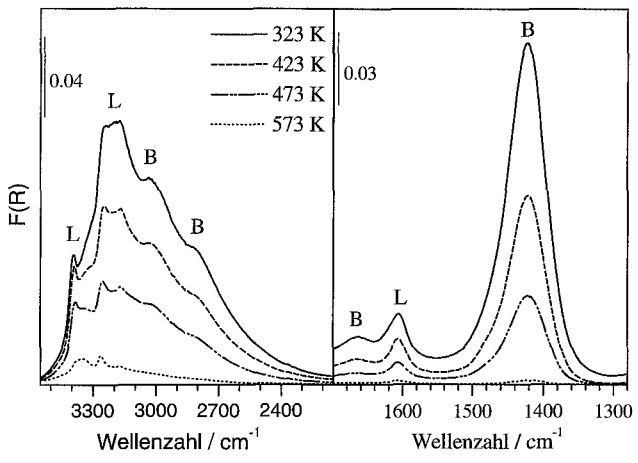

FIG. 5. SCR-TPD experiment carried out on WO_3–V_2O_5/TiO_2 catalyst 5W/3V monitored by DRIFTS. Sample was previously calcined *in situ* at 723 K in flowing O_2/Ar (7.2). Desorption in flowing Ar after exposure to SCR-feed up to 573 K and cooling to 323 K. Brønsted and Lewis sites are designated as B and L, respectively, according to (26, 28). The spectra are displayed in Kubelka–Munk units after subtraction of the corresponding catalyst background spectra.

to SCR feed gas (SCR-TPD, catalyst previously treated in SCR feed up to 573 K) and subsequent purging in Ar. At 323 K only weak bands due to Lewis bound ammonia (L) were observed, whereas bands indicative of Brønsted bound ammonia (B) were prominent. With increasing temperature mainly the Brønsted band decreased in intensity up to 473 K. At 573 K only weak bands due to Lewis bound ammonia remained.

Influence of calcination temperature on type of hydroxyl group. The DRIFT spectra in Fig. 6 show the bands associated with hydroxyl groups which are consumed during the adsorption of ammonia on the catalysts. In panel A, catalysts derived from WO_3/TiO_2, calcined at 573 or 1023 K before the grafting of vanadia, are compared. Catalyst $5W_{1023}/1V$ showed a new V–OH band at 3597 cm^{-1}, whereas the bands around 3646 cm^{-1} of V–OH groups are less intense than those for 5W/1V (13). In panel B, catalyst WVWVW/V is compared after *in situ* calcination at 573 and 723 K, respectively. Catalyst $WVWVW/V_{723}$, calcined at 723 K, also showed a new V–OH band at 3598 cm^{-1}, and bands around 3646 cm^{-1} were less intense than those for WVWVW/V.

3.2.3. Temperature-Programmed Reduction with NH_3

To elucidate a possible correlation between the catalytic activity and the reducibility by ammonia, some catalysts were investigated by means of NH_3-TPR. Comparing 5W/1V and $5W_{1023}/1V$ (with the same vanadia loading per surface area) reveals that N_2 production, indicative for reduction of the catalyst by NH_3, set in at lower temperature

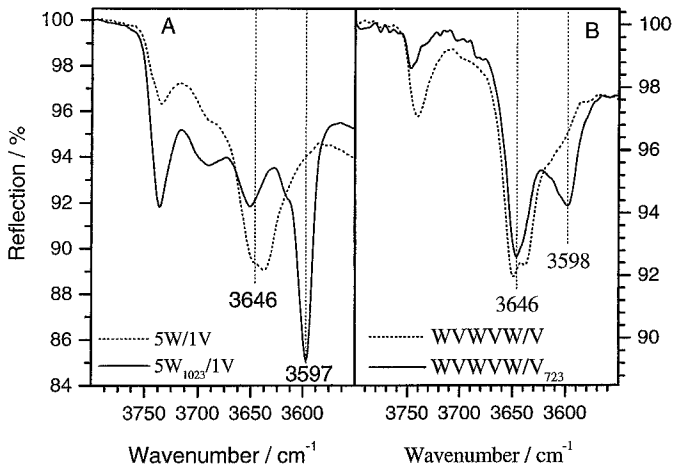

FIG. 6. Acidic hydroxyl groups on V_2O_5–WO_3/TiO_2 catalysts probed by ammonia adsorption. The ν(OH) stretching region of the diffuse reflectance FTIR (DRIFT) spectra is displayed. The OH-bands consumed by ammonia adsorption (background: catalysts before adsorption) are shown. (A) Comparison of singly vanadia-grafted WO_3/TiO_2 catalysts where the WO_3/TiO_2 precursor was calcined at 573 and 1023 K, respectively. Samples were previously calcined *in situ* at 573 K in O_2/Ar (7%). (B) Comparison of catalyst WVWVW/V after *in situ* calcination in O_2/Ar (7%) at 573 and 723 K, respectively.

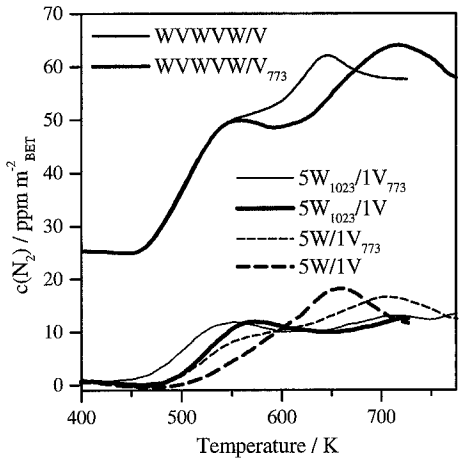

FIG. 7. TPR profiles of V_2O_5–WO_3/TiO_2 catalysts reduced by NH_3. Samples were previously calcined *in situ* in flowing O_2/He (7.2%) for 3 h at 573 and 773 K, respectively. TPR in flowing NH_3/He (3600 ppm); heating rate, 10 K/min. N_2 concentrations are referred to the total surface area (BET) of the samples. Sample designations are explained under Experimental.

for $5W_{1023}/1V$. For both catalysts, higher calcination temperature (773 K) led to a similar shift of the onset of reduction to lower temperature (Fig. 7). For $5W/1V_{773}$ and $5W_{1023}/1V$, the same onset temperature was observed, but for the latter the reduction at $T < 600$ K was more intense. Between 600 and 680 K the highest rate of reduction was observed for 5W/1V, and above 680 K the highest rate was observed for $5W/1V_{773}$. N_2-production curves of WVWVW/V after calcination at 573 and 773 K coincided below 550 K, but they became very different at higher temperature.

3.2.4. Time of Flight Secondary Ion Mass Spectrometry

To gain structural information concerning the possible presence of vanadia–tungsta connectivities, i.e., the presence of V–O–W bridges, secondary ion mass spectra were recorded for catalysts 4V, 5W, $5W/3V_{773}$, and $5W_{1023}/3V$. Whereas no relevant information could be obtained from the positive spectra, the negative spectra provided valuable insight into catalyst surface composition.

Measurements on four different samples of catalyst $5W_{1023}/3V$ afforded virtually the same spectra, indicating the homogeneity of the catalyst surface.

Figure 8A shows the relevant part of the TOF-SIMS spectrum of 5W, with major peaks at $m/z = 327$, 328, 329, and 331. Minor peaks were found at $m/z = 325$, 326, and 330. Other peaks in this region were not significantly higher than the background noise. For $5W/3V_{773}$ (Fig. 8B) four major peaks were observed, at $m/z = 329$, 330, 331, and 333, as well as minor peaks at $m/z = 327$, 328, 332, and 334. Similar peaks were found for catalyst $5W_{1023}/3V$. For 4V no such peaks occurred. The different peak positions for the ternary catalyst compared to those of the binary catalysts

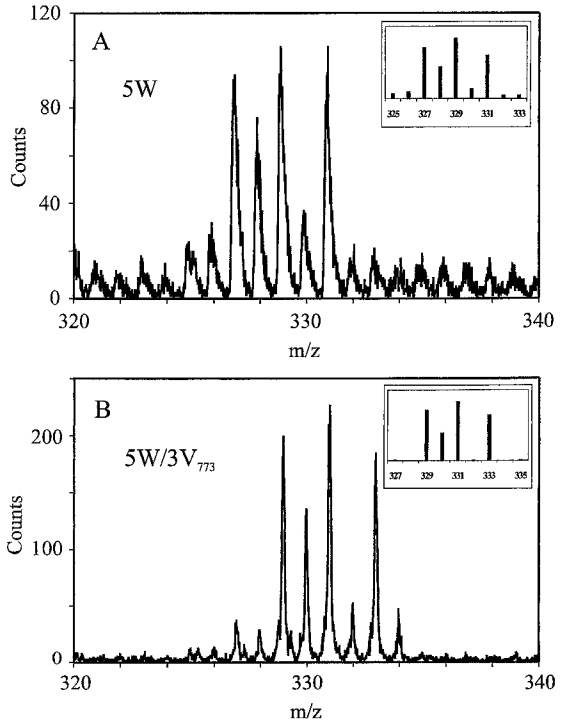

FIG. 8. Negative TOF-SIMS spectra in the $m/z = 320$–340 region for (A) WO_3/TiO_2 (5W) and (B) V_2O_5–WO_3/TiO_2 (5W/3V_{773}) catalysts. Conditions are explained under Experimental.

indicate that the ternary catalyst contains different surface species than the binary catalysts, which will be discussed in Section 4.2.

4. DISCUSSION

The SCR-TPD results will be discussed first, because they are used in the succeeding discussion of the interrelation between catalytic activity and surface chemical properties.

4.1. Temperature-Programmed Desorption (SCR-TPD)

For the binary WO_3/TiO_2 catalysts NH_3 desorption was observed up to highest temperature, indicating the strongest Lewis sites for these catalysts (28). Assuming an even distribution of tungsta over the titania surface, the constantly decreasing intensity of the N_2 desorption at 400 K with increasing tungsta loading (Fig. 1) indicates a progressive coverage of the titania surface. For 5W the N_2 evolution was 10% of that for the pure support, suggesting that about 10% of the titania surface was still uncovered.

For the multiply grafted V_2O_5/TiO_2 and ternary catalysts, N_2 and NO evolution occurred around 415 K (Figs. 2–4). Such an evolution can be explained by oxidation of adsorbed NH_3 or stabilization of NO–NH_3 reaction intermediates at room temperature on the catalyst surface. Because such an evolution was not observed in NH_3-TPD experiments (21, 25, 29), it is probably due to decomposition of a reaction intermediate. For WO_3/TiO_2 no N_2 or NO evolution was observed around 415 K, indicating that WO_3/TiO_2 catalysts can not stabilize a reaction intermediate as observed with the other catalysts.

On singly vanadia-grafted binary and ternary catalysts ammonia desorption was dominant at high temperature ($T > 500$ K, Figs. 2–4), whereas on the high loaded V_2O_5/TiO_2 and ternary catalysts predominantly NH_3 desorption from weaker acid sites was observed with desorption maxima at 400 K and ca. 490 K (Figs. 2–4). The second maximum is assigned to desorption from Brønsted acid sites as indicated by the comparison of different TPD experiments (25, 29). The first maximum can be attributed to NH_3 desorbing from either Brønsted or Lewis sites (25, 28–30), which cannot be distinguished from SCR-TPD alone. The DRIFT spectra for 5W/3V (Fig. 5) indicated that under SCR-TPD conditions NH_3 desorbs also at 400 K, predominantly from Brønsted acid sites. Lewis acid sites can be converted into Brønsted acid sites through adsorption of water, which is present as a reaction product in the SCR reaction even at room temperature for catalysts in this study. Experiments concerned with the adsorption of water on catalysts with preadsorbed NH_3 showed the transformation of Lewis bound into Brønsted bound ammonia (25, 29). The transformation of Lewis sites into Brønsted sites can consequently also occur when these sites have been already covered by ammonia.

The SCR-TPD profiles changed after the grafting of vanadia, but differed only slightly after the grafting with tungsta. In line with this, SCR-TPD profiles of high loaded ternary catalysts resembled those measured for V_2O_5/TiO_2. Thus we conclude that the surface acidity of the ternary catalyst is mainly influenced by vanadium oxide.

4.2. Interrelation between Catalytic Activity and Surface Chemical Properties

For binary and ternary catalysts of low loading and with low intrinsic activity (TOF < 0.3 NO/(V*ks), Tables 1–3), ammonia desorbed predominantly at high temperatures ($T >$ ca. 500 K, Figs. 2–4) and the N_2 and NO desorptions due to reaction intermediates were very weak and occurred at relative high temperature (maximum at ca. 450 K). For catalysts with high intrinsic activity (TOF > 0.3 NO/(V*ks), Tables 1–3), NH_3 desorption at high temperature was less prominent and desorption at low temperature was enhanced; N_2 and NO desorption occurred at ca. 415 K and was more pronounced (Figs. 2–4). These effects, especially illustrated by comparing catalysts 2W/1V and 2W_{1023}/1V (Table 2 and Fig. 3), with the same vanadia loading per surface area, indicate the importance of weak acid sites for SCR-DeNO_x.

Increasing the calcination temperature from 573 to 773 K resulted in a shift of the high-temperature NH_3 desorption

maximum to lower temperature for catalysts with significantly enhanced intrinsic activity (30% or more, TOF in Tables 1–3). For catalysts with unchanged intrinsic activity, no shift was observed, and for catalysts with decreased activity, a shift to higher temperature was observed, further supporting the correlation between activity and weak acid sites.

The triply grafted ternary catalysts 2W/1V, WV/W, and 3(W + V), which exhibited similar DRIFT spectra (13), also showed similar SCR-TPD profiles (Figs. 3 and 4). Comparable profiles were also observed for the quadruply grafted catalysts with virtual the same vanadia and tungsta loading and about monolayer coverage (2V/2W, 2W/2V, and WVW/V). Also, their activities were not significantly different and did not change markedly when the calcination temperature was increased to 773 K (Tables 1–3). Thus no influence of the preparation sequence at monolayer coverage was observed on the catalyst properties, when similar vanadia and tungsta loading were present.

For catalysts with a total loading of less than a monolayer (three graftings) a decrease in intrinsic activity was observed when the calcination temperature was raised to 773 K (Tables 1–3). This can be explained by the spreading of vanadia over the titania surface (31). Machej *et al.* (32) observed the disappearance of V_2O_5 crystallites at 723 K, which were still present after calcination at 673 K. Although the microscopic mechanism of "solid–solid wetting" is still not understood in detail, the phenomenon is attributed to a minimization of surface free energy (33). Thus vanadia can migrate over the surface and polymeric vanadates are transformed into monomeric vanadyl species, which are less active (34, 35). Migration on the free titania surface is preferred, because titania possesses a higher surface free energy than tungsta (28–38 and 10 $\mu J/cm^2$, respectively (33)). A decrease of the polymeric species with increasing temperature was also observed in the Raman spectra for the present catalysts (36). The high activation energy for the low loaded ternary catalysts (ca. 80 kJ/mol, Tables 2 and 3) compared to that of the V_2O_5/TiO_2 catalysts hints toward an interaction between both oxides. After calcination at 773 K the activation energy was (ca. 70 kJ/mol) only slightly higher than that for the V_2O_5/TiO_2 catalysts, thus indicating less interaction between both oxides. Thus a breaking of possible V–O–W bridges due to spreading of vanadia could result in decreased activity.

For catalysts with monolayer coverage free space is no longer available on the titania surface. Thus the migration of vanadium oxide is hindered and no similar restructuring can occur, which could explain the observed unchanged activity (Tables 1–3), activation energy, and SCR-TPD profiles.

At loadings higher than a monolayer an increase of the activity with the calcination temperature was observed (Tables 1–3). The higher calcination temperature seems to intensify the interaction between vanadia and tungsta. Thus for catalysts 5W/3V and WVWVW/V new species were formed which possess hydroxyl groups with a characteristic frequency $\leq 3600\ cm^{-1}$ (Fig. 6). Such hydroxyls were not observed for V_2O_5/TiO_2 (13). Interestingly, with the formation of the new species the activation energy decreased compared to that of V_2O_5/TiO_2 catalysts (Tables 1–3). Similar differences were observed comparing 5W/1V and $5W_{1023}$/1V, the latter being three times more active (Table 2) and possessing hydroxyl groups characterized by a band at $3597\ cm^{-1}$ (Fig. 6). These results corroborate the importance of Brønsted acidity for SCR-DeNO_x (37–39).

Comparing the ternary catalysts 5W/1V and $5W_{1023}$/1V, the latter being three times more active than the former (Table 2), no difference in the reduction of vanadia by hydrogen was observed (13). NH_3-TPR (Fig. 7) showed reduction of the more active catalyst at lower temperature. However, increasing the calcination temperature to 773 K led to a similar shift of the reduction to lower temperature for both catalysts (Fig. 7), although the activity doubled for 5W/1V, but did not increase significantly for $5W_{1023}$/1V (Table 2). For WVWVW/V no difference in the NH_3-TPR up to 550 K was observed for either calcination temperature (Fig. 7), although the activity increased by 50% upon raising the calcination temperature (Table 3). Between 550 K and 650 K the reduction rate of WVWVW/V calcined at 573 K was even higher (Fig. 7). From these results no correlation is apparent between the ease of reduction of the catalysts by hydrogen or ammonia and the activity.

Substances with one tungsten atom give rise in TOF-SIMS measurements to a characteristic pattern of four peaks due to the four main tungsta isotopes ^{182}W, ^{183}W, ^{184}W, and ^{186}W. Consequently, such a pattern could not be identified for V_2O_5/TiO_2. For the WO_3/TiO_2 catalyst 5W the four characteristic peaks at $m/z = 327, 328, 329$, and 331 can be assigned to $[W^{6+}\ Ti^{4+}\ O_6^{2-}\ H^+]^-$. A calculated isotopic pattern for $[WTiO_6H]^-$ can be seen as an inset in Fig. 8A.

For the ternary V_2O_5–WO_3/TiO_2 catalyst $5W/3V_{773}$ and $5W_{1023}$/3V a similar pattern was found in the same region, but shifted by two m/z numbers compared to 5W. The pattern can be explained by an overlap of the spectra of $[W^{6+}\ V^{5+}\ O_6^{2-}]^-$, $[W^{5+}\ V^{5+}\ O_6^{2-}\ H^+]^-$, or $[W^{6+}\ V^{4+}\ O_6^{2-}\ H^+]^-$ and the above-mentioned $[W^{6+}\ Ti^{4+}\ O_6^{2-}\ H^+]^-$, the contribution of the first cluster-ion being the most important. The inset in Fig. 8B shows the isotopic pattern of this ion. The peaks at $m/z = 327$ and 328 can be asigned to $[WTiO_6H]^-$, those at $m/z = 332$ and 334 to $[WVO_6H]^-$. This type of cationization by addition of a proton is very common in TOF-SIMS experiments. The identified $[WVO_6]^-$ cluster ions clearly indicate the presence of W–O–V connectivities on the catalyst surface of the ternary catalysts $5W/3V_{773}$ and $5W_{1023}$/3V.

Tran *et al.* (40) found that the highest occupied molecular orbital of pseudotetrahedral oxovanadium groups ($-O_3V{=}O$) is a nonbonding a_2 symmetry orbital localized on the basal plane ligands. This is in line with the suggestion

of Deo *et al.* (41) that the bridging oxygens must be responsible for substrate effects. The possibility that the basal plane ligands can exert a strong effect on the metal center has been discussed in detail by Feher *et al.* (42). The interaction between vanadia and tungsta observed in this and other studies (13, 43, 44) may occur through oxygen bridging of polyhedra and/or through the conduction band of TiO_2 (43). Alemany *et al.* (43) interpreted for high loaded ternary catalysts a shift to higher frequency of the IR band at 700 cm^{-1}, which is associated with W_xO_y species, as slight evidence for the presence of mixed $W_xV_yO_z$ species. Also, grafting, DRIFT, and XPS data suggested the formation of bridging oxygen between V and W (13). To our knowledge, the present TOF-SIMS measurements provide for the first time direct evidence for the existence of V–O–W bridging bonds which can explain the higher activity of ternary catalysts compared to binary V_2O_5/TiO_2 catalysts.

5. CONCLUSIONS

The influence of the sequence of grafting steps on the surface chemical properties and catalytic activity of ternary V_2O_5–WO_3/TiO_2 catalysts, prepared by the grafting of V- and W-alkoxides on a TiO_2 support, has been investigated. TPD and DRIFTS studies and catalytic measurements of SCR of NO by NH_3 showed that the surface chemical properties and the activity of the catalysts were independent of the sequence of grafting steps up to an experimental monolayer for catalysts with comparable composition. Increase of the calcination temperature from 573 to 773 K resulted in lower activity for loadings of less than a monolayer. This is traced to the spreading of the vanadia species leading to an increased population of the less active monomers. At monolayer coverage no spreading can occur due to lack of free titania surface; thus no difference in activity was observed when the calcination temperature was increased. At loading higher than a monolayer the interaction between vanadia and tungsta species is intensified with higher calcination temperature, affording new species with hydroxyl groups characterized by a vibrational band at a frequency lower than 3600 cm^{-1} and higher activity. This corroborates the important role of Brønsted sites in SCR-DeNO_x.

The formation of weaker acid sites from which ammonia desorbs at temperatures <500 K and activity seem to be related, whereas no correlation could be found between activity and the ease of reduction of the catalysts by hydrogen or ammonia. The surface acidity seems to be mainly influenced by vanadium oxide.

TOF-SIMS measurements indicated that V–O–W connectivities are present on the ternary catalysts. Thus V and W interact directly through an oxygen bridge, resulting in a higher activity compared to the binary catalysts.

Highest turnover frequencies and lowest activation energies resulted when (i) vanadia and tungsta were present on the catalyst, (ii) the loading exceeded an experimental monolayer, and (iii) WO_3/TiO_2 was calcined at 1023 K before vanadia deposition or the final V_2O_5–WO_3/TiO_2 catalyst was calcined at 773 K.

ACKNOWLEDGMENTS

We thank Dr. M. Textor for help in the TOF-SIMS measurements and for valuable discussions. Financial support by the Swiss National Science Foundation is kindly acknowledged.

REFERENCES

1. Bosch, H., and Janssen, F., *Catal. Today* **2**, 369 (1988).
2. Bond, G. C., and Tahir, S. F., *Appl. Catal.* **71**, 1 (1991).
3. Sloss, L. L., "Nitrogen Oxide Control Technology Fact Book." Noyes Data Corporation, Park Ridge, 1992.
4. Busca, G., Lietti, L., Ramis, G., and Berti, F., *Appl. Catal. B* **18**, 1 (1998).
5. Parvulescu, V. I., Grange, P., and Delmon, B., *Catal. Today* **46**, 233 (1998).
6. Amiridis, M. D., and Solar, J. P., *Ind. Eng. Chem. Res.* **35**, 978 (1996).
7. Ramis, G., Busca, G., and Forzatti, P., *Appl. Catal. B* **1**, L9 (1992).
8. Vuurman, M. A., Wachs, I. E., and Hirt, A. M., *J. Phys. Chem.* **95**, 9928 (1991).
9. Mastikhin, V. M., Terskikh, V. V., Lapina, O. B., Filimonova, S. V., Seidl, M., and Knözinger, H., *J. Catal.* **156**(1), 1 (1995).
10. Kijenski, J., Baiker, A., Glinski, M., Dollenmeier, P., and Wokaun, A., *J. Catal.* **101**, 1 (1986).
11. Handy, B. E., Baiker, A., Schraml-Marth, M., and Wokaun, A., *J. Catal.* **133**, 1 (1992).
12. Baiker, A., Dollenmeier, P., Glinski, M., and Reller, A., *Appl. Catal.* **35**, 351 (1987).
13. Reiche, M. A., Bürgi, T., Scholz, A., Schnyder, B., Wokaun, A., and Baiker, A., *Appl. Catal. A* **198**, 155 (2000).
14. Weisz, P. B., and Prater, C. D., *Adv. Catal.* **6**, 143 (1954).
15. Schneider, M., Maciejewski, M., Tschudin, S., Wokaun, A., and Baiker, A., *J. Catal.* **149**, 326 (1994).
16. Went, G. T., Leu, L.-J., and Bell, A. T., *J. Catal.* **134**, 479 (1992).
17. Wachs, I. E., *Catal. Today* **27**, 437 (1996).
18. Vermaire, D. C., and Berge, P. C. v., *J. Catal.* **116**, 309 (1989).
19. Bond, G. C., Flamerz, S., and Wijk, L. v., *Catal. Today* **1**, 229 (1987).
20. Bond, G. C., Zurita, J. P., Flamerz, S., Gellings, P. J., Bosch, H., Ommen, J. v., and Kip, B. J., *Appl. Catal.* **22**, 361 (1986).
21. Baiker, A., Handy, B., Nickl, J., Schraml, M., and Wokaun, A., *Catal. Lett.* **14**, 89 (1992).
22. Engweiler, J., and Baiker, A., *Appl. Catal. A Gen.* **120**, 187 (1994).
23. Hu, S., and Apple, T. M., *J. Catal.* **158**, 199 (1996).
24. Engweiler, J., Harf, J., and Baiker, A., *J. Catal.* **159**, 259 (1996).
25. Reiche, M., Ph.D. Thesis No. 13155, Swiss Federal Institute of Technology, ETH, Zürich, Switzerland, 1999.
26. Ramis, G., Yi, L., and Busca, G., *Catal. Today* **28**, 373 (1996).
27. Amores, J. M. G., Escribano, V. S., Ramis, G., and Busca, G., *Appl. Catal. B* **13**, 45 (1997).
28. Reiche, M. A., Ortelli, E., and Baiker, A., *Appl. Catal. B* **23**, 187 (1999).
29. Reiche, M., and Baiker, A., unpublished results.
30. Pinaeva, L. G., Suknev, A. P., Budneva, A. A., Paukshtis, E. A., and Bal'zhinimaev, B. S., *J. Mol. Catal.* **112**, 115 (1996).
31. Haber, J., Machej, T., and Czeppe, T., *Surf. Sci.* **151**, 301 (1985).
32. Machej, T., Haber, J., Turek, A. M., and Wachs, I. E., *Appl. Catal.* **70**, 115 (1991).
33. Leyrer, J., Margraf, R., Taglauer, E., and Knözinger, H., *Surf. Sci.* **201**, 603 (1988).

34. Went, G. T., Leu, L.-J., Rosin, R., and Bell, A. T., *J. Catal.* **134**, 492 (1992).
35. Baiker, A., *Chimia* **50**(3), 65 (1996).
36. Scholz, A., Dissertation ETH-No. 12640, Federal Institute of Technology, Zürich, Switzerland, 1998.
37. Topsøe, N. Y., Dumesic, J. A., and Topsoe, H., *J. Catal.* **151**, 241 (1995).
38. Nickl, J., Dutoit, D., Baiker, A., Scharf, U., and Wokaun, A., *Ber. Bunsenges. Phys. Chem.* **97**, 217 (1993).
39. Chen, J. P., and Yang, R. T., *Appl. Catal.* **80**, 135 (1992).
40. Tran, K., Hanning-Lee, M. A., Biswas, A., Stiegman, A. E., and Scòtt, G. W., *J. Am. Chem. Soc.* **117**, 2618 (1995).
41. Deo, G., and Wachs, I. E., *J. Catal.* **129**, 307 (1991).
42. Feher, F. J., and Walzer, J. F., *Inorg. Chem.* **30**, 1689 (1991).
43. Alemany, L. J., Lietti, L., Ferlazzo, N., Forzatti, P., Busca, G., Giamello, E., and Bregani, F., *J. Catal.* **155**, 117 (1995).
44. Lietti, L., Forzatti, P., and Bregani, F., *Ind. Eng. Chem. Res.* **35**, 3884 (1996).